Struct. Cell. Biochem. 16, 91-103.
Gentner, N. E., Rözga, B., Smith, B. P., Paterson, M. C., & Cadet, J. (1981) *Proceedings of the 9th Annual Meeting of the American Society for Photobiology*, p 164, Pergamon, Oxford, U.K.
Gentner, N. E., Weinfeld, M., Johnson, L. D., & Paterson, M. C. (1984) *Environ. Mutagen. 6*, 429.
Haseltine, W. A., Gordon, L. K., Lindan, C. P., Grafstrom, R. H., Shaper, N. L., & Grossman, L. (1980) *Nature (London) 285*, 634-641.
Jagger, J. (1967) in *Introduction to Research in Ultraviolet Photobiology*, pp 137-139, Prentice-Hall, Englewood Cliffs, NJ.
La Belle, M., & Linn, S. (1982) *Photochem. Photobiol. 36*, 319-324.
Lindahl, T. (1982) *Annu. Rev. Biochem. 51*, 61-87.
Nakabeppu, Y., & Sekiguchi, M. (1981) *Proc. Natl. Acad. Sci. U.S.A. 78*, 2742-2746.
Niggli, H. J., & Cerutti, P. A. (1983) *Biochemistry 22*, 1390-1395.
Paterson, M. C. (1986) in *Biochemical and Molecular Epidemiology of Human Cancer* (Harris, C. C., Ed.) Liss, New York (in press).
Paterson, M. C., & MacFarlane, S. J. (1983) *Radiat. Res. 94*, 664.
Paterson, M. C., Gentner, N. E., Middlestadt, M. V., & Weinfeld, M. (1984) *J. Cell. Physiol., Suppl. 3*, 45-62.
Paterson, M. C., Gentner, N. E., Middlestadt, M. V., Mirzayans, R., & Weinfeld, M. (1985) in *Epidemiology and Quantitation of Environmental Risk in Humans from Radiation and Other Agents* (Castellani, A., Ed.) pp 235-267, Plenum, New York.
Radany, E. H., & Friedberg, E. C. (1980) *Nature (London) 286*, 182-185.
Regan, J. D., Trosko, J. E., & Carrier, W. L. (1968) *Biophys. J. 8*, 319-325.
Sancar, A., & Rupp, W. D. (1983) *Cell (Cambridge, Mass.) 33*, 249-260.
Sancar, A., Smith, F. W., & Sancar, G. B. (1984) *J. Biol. Chem. 259*, 6028-6032.
Schneider, E. L., Stanbridge, E. J., & Epstein, C. J. (1974) *Exp. Cell Res. 84*, 311-318.
Setlow, R. B. (1966) *Science (Washington, D.C.) 153*, 379-386.
Setlow, R. B., Carrier, W. L., & Bollum, F. J. (1964) *Biochim. Biophys. Acta 91*, 446-461.
Setlow, R. B., Regan, J. D., & Carrier, W. L. (1969) *Proc. Natl. Acad. Sci. U.S.A. 64*, 1035-1041.
Smith, C. A., & Okumoto, D. S. (1984) *Biochemistry 23*, 1383-1391.
Sober, H. A., Ed. (1968) *Handbook of Biochemistry: Selected Data for Molecular Biology*, 2nd ed., pp H1-H65, The Chemical Rubber Co., Cleveland, OH.
Sutherland, B. M. (1978) in *DNA Repair Mechanisms* (Hanawalt, P. C., Friedberg, E. C., & Fox, C. F., Eds.) pp 113-122, Academic Press, New York.
Weinfeld, M., Gentner, N. E., Johnson, L. D., & Paterson, M. C. (1984) *Proceedings of the 75th Annual Meeting of the American Association for Cancer Research*, p 105, Waverly, Baltimore, MD.

Characteristics and Variations of B-Type DNA Conformations in Solution: A Quantitative Analysis of Raman Band Intensities of Eight DNAs†

Roger M. Wartell* and Juan T. Harrell
Schools of Physics and Biology, Georgia Institute of Technology, Atlanta, Georgia 30332
Received September 16, 1985; Revised Manuscript Received December 16, 1985

ABSTRACT: Raman spectra were obtained from four bacterial DNAs varying in GC content and four periodic DNA polymers in 0.1 M NaCl at 25 °C. A curve fitting procedure was employed to quantify and compare Raman band characteristics (peak location, height, and width) from 400 to 1600 cm^{-1}. This procedure enabled us to determine the minimum number of Raman bands in regions with overlapping peaks. Quantitative comparison of the Raman bands of the eight DNAs provided several new results. All of the DNAs examined required bands near 809 (±7) and 835 (±5) cm^{-1} to accurately reproduce the experimental spectra. Since bands at these frequencies are associated with A-family and B-family conformations, respectively, this result indicates that all DNAs in solution have a mixture of conformations on the time scale of the Raman scattering process. Band characteristics in the 800–850-cm^{-1} region exhibited some dependence on CG content and base pair sequence. As previously noted by Thomas and Peticolas [Thomas, G. A., & Peticolas, W. L. (1983) *J. Am. Chem. Soc. 105*, 993], the poly[d(A)]·poly[d(T)] spectra were qualitatively distinct in this region. The A-family band is clearly observed at 816 cm^{-1}. The intensity of this band and that of the B-family band at 841 cm^{-1} were similar, however, to intensities in the natural DNA spectra. Three bands at 811, 823, and 841 cm^{-1} were required to reproduce the 800–850-cm^{-1} region of the poly[d(A-T)]·poly[d(A-T)] spectra. This may indicate the presence of three backbone conformations in this DNA polymer. Analysis of intensity vs. GC content for 42 Raman bands confirmed previous assignments of base and backbone vibrations and provided additional information on a number of bands.

Several investigations have shown that the structure of duplex DNA is influenced by its base pair sequence and environment. X-ray diffraction studies on DNA crystals have demonstrated three classes of DNA structures, A, B, and Z (Rich et al., 1981; Dickerson et al., 1982; Shakked et al., 1983). Small localized alterations were observed within each type or family of DNA structure (Wang et al., 1980; Drew

† This work was supported by the National Institutes of Health (GM33543).

0006-2960/86/0425-2664$01.50/0

et al., 1981; Milane et al., 1984). In solution, DNA is subject to a variety of internal motions and environmental influences that, in general, can not be recreated in the solid state. These factors can be expected to produce conformations that are more varied and potentially different from structures observed in the solid state. The dynamic character of DNA is indicated by fluctuational base pair opening (Englander & Kallenbach, 1983; Mirau & Kearns, 1985; Wartell & Benight, 1982) and topological, bending, and torsional considerations (Klysik et al., 1981; Hagerman, 1981; Shore & Baldwin, 1983; Horowitz & Wang, 1984). NMR studies showed that the same DNA molecule does not necessarily have the same average solution and solid-state structures (Reid et al., 1983; Sarma et al., 1985).

Raman spectroscopy is one of several techniques that can be employed to investigate DNA conformation in solution. It has the advantage of being applicable to both large and small nucleic acids. The complexity of DNA Raman spectra has necessitated that an empirical approach be employed in assigning Raman bands to specific molecular groups and conformations. Studies on model compounds (Lord & Thomas, 1967; Thomas & Kyogoku, 1977; Nishimura et al., 1978, 1984) and DNA fibers and crystals (Erfurth et al., 1975; Thomas & Peticolas, 1983a; Martin & Wartell, 1982; Thomas et al., 1984) have been of great value in establishing assignments of DNA Raman bands. The three structural classes of DNA, A, B, and Z, can be distinguished by their Raman vibrational spectra.

In order to establish a basis for examining possible sequence-dependent variations in DNA Raman bands, we examined the Raman spectra of eight DNAs in 0.1 M NaCl solution at 25 °C. Four of the DNAs were heterogeneous-sequence naturally occurring DNAs varying in percent GC from 26.5 to 72%. The other four DNAs were synthetic DNA polymers. A curve fitting procedure was applied to quantify Raman band characteristics (peak location, height, and width) from 400 to 1600 cm^{-1}. This allowed us to examine the effect of percent GC content and base pair sequence on the intensities of previously assigned base and backbone vibrations. We have confirmed many assignments and obtained additional information on several Raman bands.

This study also provided new results on several aspects of DNA conformation in solution. Evidence is given for the presence of C3′-endo and C2′-endo family backbone bands in all DNA spectra. The quantitative analysis of the synthetic DNAs' spectra revealed features relating to their conformation. Studies on these polymers have been previously reported (Pohl et al., 1973; Thomas & Peticolas, 1983b; Fidor et al., 1984; Thomas & Benevidis, 1985; Wartell et al., 1983).

Material and Methods

Samples. The four naturally occurring DNAs used in the study were purchased from Sigma Chemical Co. They were from the bacteria *Clostridium perfringens* (26.5% GC), *Bacillus subtilis* (44% GC), *Escherichia coli* (50% GC), and *Micrococcus luteus* (72% GC). They were extracted with phenol–chloroform and dialyzed into 10 mM NaCl + 0.1 mM ethylenediaminetetraacetic acid (EDTA). The DNAs were then precipitated with 2–3 volumes of ethanol at −70 °C, backwashed with 75% ethanol twice to remove excess salts, and lyophilized to dryness. Gellike solutions were prepared for Raman experiments by adding 0.1 M NaCl to give concentrations at about 40–80 mg/mL. The synthetic DNAs poly[d(A-T)]·poly[d(A-T)], poly[d(A)]·poly[d(T)], and poly [d(G-C)]·poly[d(G-C)] were purchased from P-L Biochemicals. They were prepared for Raman spectroscopy in a manner similar to that described above. All DNAs were characterized by their UV spectra and DNA denaturation curve in 0.1 M NaCl + 1 mM sodium phosphate (pH 7.) + 0.1 mM EDTA except for poly[d(G-C)]·poly[d(G-C)]. This DNA was melted in 5 mM Na^+. Poly[d(T-G)]·poly[d(C-A)] was generously provided by Dr. J. Alderfer.

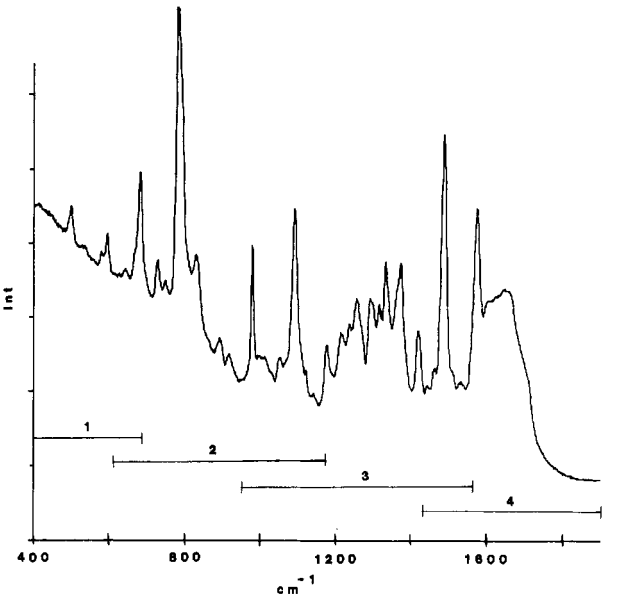

FIGURE 1: Raman spectra of *M. luteus* DNA is shown from 400 to 1850 cm^{-1}. The four regions designated below the spectra were the intervals employed in the quantitative analyses of the Raman band characteristics. The broad water band at 1645 cm^{-1} made the evaluation of nearby bands unreliable.

Raman Measurements. Spectra were obtained by using the 514.5-nm line of an argon ion laser. Laser power of 150–200 mW was employed to record spectra between 400 and 1900 cm^{-1}. The effective slit width of the spectrometer was 4.0 cm^{-1}. Scanning of the spectrometer (Spex 1401) and photon counting from the photomultiplier (RCA 31034) were coordinately controlled by a Tektronix 4051 computer. Sample volumes of 5–10 μL were placed in quartz capillary cells and held against an aluminum block whose temperature could be controlled by circulating water. All spectra were obtained at 25 °C.

Figure 1 shows a typical Raman spectrum from this study. It is the result of four consecutive scans with counts accumulated for 2 s/cm^{-1}. At least two separate spectra were taken of each sample. Band peak heights, widths, and locations were evaluated by a nonlinear least-squares curve fitting procedure. The procedure is based on the Marquardt (1964) algorithm and has been briefly described previously (Wartell et al., 1983). A polynomial up to order seven represented the background. Raman bands were reproduced by employing Lorentzian functions convoluted with the instrument function. For a given spectral region, the number of bands, their locations, and the order of the polynomial background curve were first estimated from the experimental spectra. Widths were initially estimated as 8 or 15 cm^{-1}. On the basis of this first guess, a linear least-squares fitting program was employed to provide a first-order estimate of peak heights and background parameters. The Marquardt algorithm then iteratively refined the fit by varying peak locations, widths, and heights as well as background parameters. The algorithm stopped when specified least-squares conditions were met or when 500 iterations were reached. A copy of the program in Fortran V appropriate for the Control Data Corp. Cyber 850 computer with IMSL programs is available upon request. The curve fitting proce-

dure was applied to the four regions designated in Figure 1. These regions were large enough to follow the background accurately without exceeding the memory required to fit the experimental spectra.

Shapes of the calculated background curves were essentially the same as those of the experimental solvent spectra. Not surprisingly, background curves of overlapping regions did not splice together perfectly. An estimate of the error generated by these end effects was made by comparing Raman band characteristics evaluated from Raman peaks shared by overlapping regions. Differences were generally no larger than repeated analyses of a single region. They were included in determining average Raman band characteristics. Each spectral region was analyzed 3 times, and the band characteristics were averaged. The second region for example required 18 bands from 640 to 1150 cm^{-1}. These bands were the minimum number required to reproduce this region in the spectra of the four natural DNAs. Band positions and widths were similar among the DNAs. In some cases, small GC-dependent frequency shifts were noted (see below). Similar results were obtained in the other spectral regions. Although some of the broader calculated bands may actually result from two vibrational bands, the analysis provides a minimum set of Raman bands, which enables an accurate intensity comparison to be made in regions of overlapping peaks.

Results

Raman Spectra of Natural DNAs. A comparison of Raman spectra of the natural DNAs was made in order to verify the percent GC dependence predicted by previous band assignments. Figure 2 shows spectra of *C. perfringens* DNA, *E. coli* DNA, and *M. luteus* DNA with backgrounds subtracted. The spectra were normalized to the 1093-cm^{-1} band associated with the PO_2^- symmetric stretching mode. The narrow Raman peak at 980 cm^{-1} was from 0.02 M sodium sulfate added to the solvent. This band or "line" provided an internal frequency standard. The effect of GC content on the intensities of a number of Raman peaks can be readily observed. Examples in the 400–1200-cm^{-1} region were the intensity decreases at 669 cm^{-1} and intensity increase at 682 cm^{-1} as the percent GC increases. These changes were expected since the 669-cm^{-1} band was assigned to thymine and the 682-cm^{-1} peak was assigned to a guanine–deoxyribose mode (Hartman et al., 1973). Similarly, the 730-cm^{-1} adenine vibration and 750-cm^{-1} thymine band decreased with increasing GC content, while the 782-cm^{-1} cytosine band increased. The peak around 833 cm^{-1} has been assigned to a phosphate–deoxyribose vibration characteristic of the B-DNA conformation (Erfurth et al., 1975). Its intensity did not significantly change with increasing percent GC.

In the 1000–1800-cm^{-1} region, the 1488-cm^{-1} band increased in intensity, the 1512 cm^{-1} band decreased, and the 1420-cm^{-1} band remained approximately constant. These observations correspond with previous assignments. The 1488-cm^{-1} mode is a purine ring vibration dominated by guanine, the 1512-cm^{-1} band is assigned to an adenine vibration, and the 1420-cm^{-1} band is assigned to deoxyribosyl CH_2 groups (Prescott et al., 1984). Changes in band intensities from 1150 to 1450 cm^{-1} were more difficult to assess. Observed peaks were the sum of contributions from overlapping Raman bands. This also occurred for the 750–840-cm^{-1} region and from 980 to 1150 cm^{-1}. In order to obtain a more quantitative comparison of Raman bands throughout the 400–1800-cm^{-1} region, we will turn to the results from the curve fitting analyses of both natural and synthetic DNAs.

Intensity vs. Percent GC of Raman Bands. Figure 3 plots

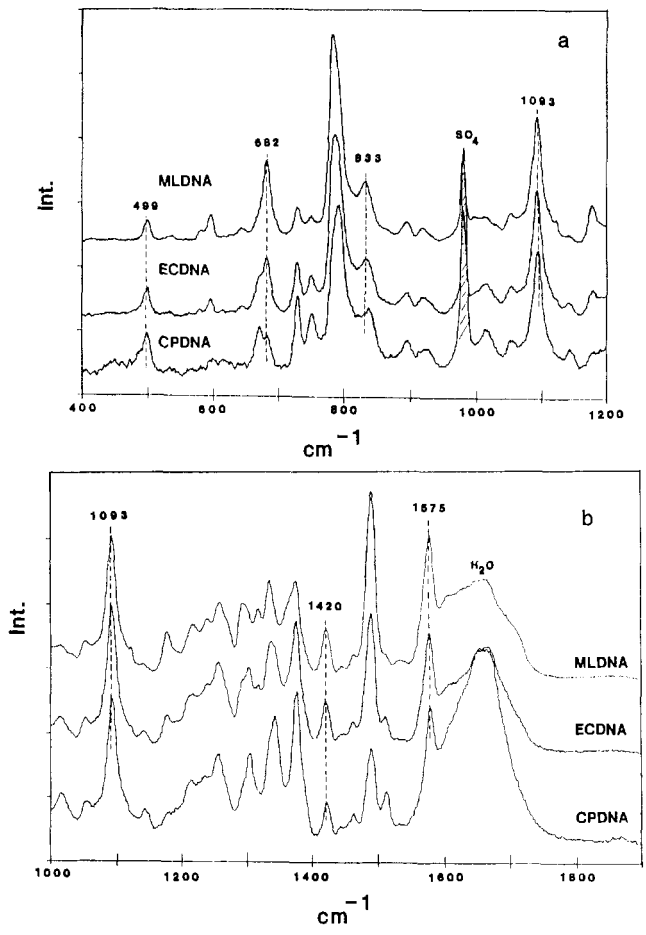

FIGURE 2: Comparison of Raman spectra of DNA from *C. perfringens* (CPDNA), *E. coli* (ECDNA), and *M. luteus* (MLDNA). Background curves were subtracted and the spectra normalized to the 1093-cm^{-1} band. (a) 400–1200-cm^{-1} region; (b) 1000–1900-cm^{-1} region.

the relative intensities of four bands from 400 to 700 cm^{-1} vs. percent GC. The filled and open symbols designate natural and synthetic DNAs, respectively. All four bands in Figure 3 have been associated with base ring vibrations. The 499-cm^{-1} band has been assigned to the sum of two vibrational modes due to guanine and thymine (Prescott et al., 1984). Our data are consistent with this assignment. Both AT DNA polymers and poly[d(G-C)]·poly[d(G-C)] have bands at 499 ± 1 cm^{-1}. In addition, the linear extrapolation of the natural DNA data indicate nonzero intensities at 0 and 100% GC. With the exception of poly[d(A-T)]·poly[d(A-T)], all the synthetic DNAs have intensity values at 499 cm^{-1} that fit the line drawn through the natural DNA data. The intensity vs. percent GC of the 596-cm^{-1} band in Figure 3 is consistent with this band being a guanine and/or cytosine vibration. Studies carried out with poly[d(I-C)]·poly[d(I-C)] and poly[d(G-meC)]·poly[d(G-meC)] indicate it is a cytosine vibration (D. Brown and R. M. Wartell, unpublished results). The GC dependence of the 669-cm^{-1} thymine band and 682-cm^{-1} guanine vibration is as anticipated. Except for slight deviations of the DNA polymers' intensities for some of the bands, the synthetic DNA data are in general accord with the linear extrapolations from the natural DNA data.

Figure 4 continues the intensity vs. percent GC plots for bands at 729, 750, 782, and 791 cm^{-1}. A small 729-cm^{-1} band for poly[d(G-C)]·poly[d(G-C)] indicates a small contribution at this frequency from a vibration not involving adenine. The 782- and 791-cm^{-1} bands form part of a convoluted set of bands from 760 to 840 cm^{-1}. This section has backbone bands

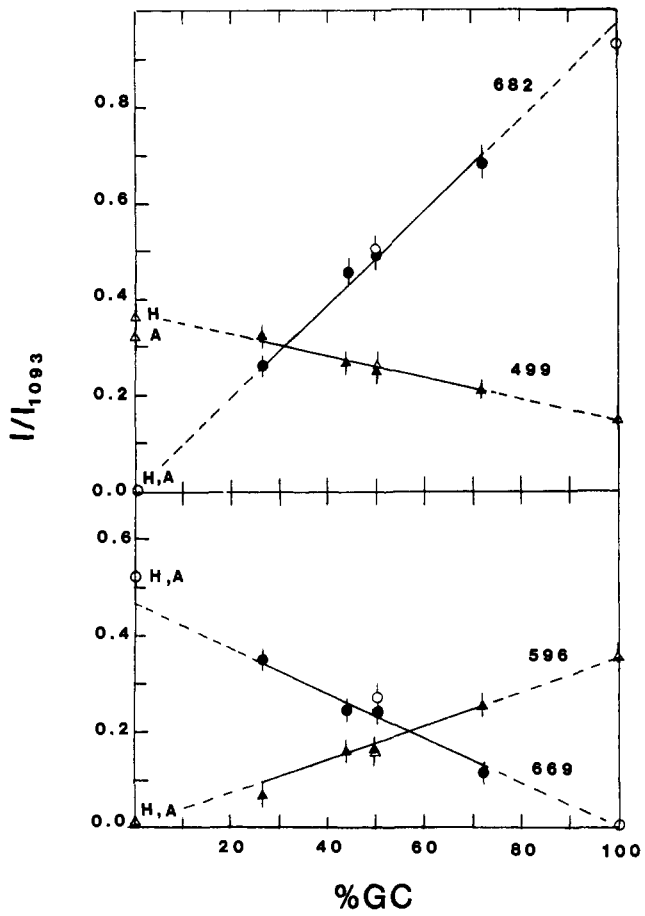

FIGURE 3: Raman intensities vs. percent GC are plotted for bands at 499, 596, 669, and 682 cm^{-1}. Filled symbols correspond to natural DNAs; open symbols are periodic DNAs. "H" refers to homopolymer AT DNA poly[d(A)]·poly[d(T)]; "A" refers to alternating AT DNA poly[d(A-T)]·poly[d(A-T)]. Intensities are relative to the 1093-cm^{-1} band.

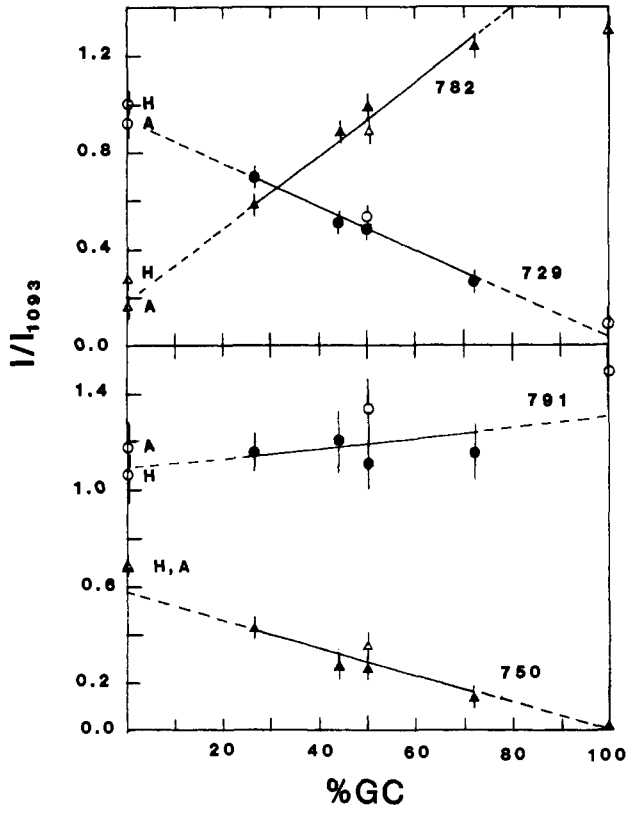

FIGURE 4: Raman intensities vs. percent GC for bands at 729, 750, 782, and 791 cm^{-1}. See Figure 3 legend for symbol description.

that show major intensity changes in the B ⇄ Z transitions. We have quantified these bands using both the 640–1150-cm^{-1} and 700–800-cm^{-1} regions. Results were similar in both cases. The 782-cm^{-1} band has been assigned to a cytosine vibration (Erfurth & Peticolas, 1975; Prescott et al., 1984). Figure 4 implies an additional contribution. Both AT DNAs require a small band around 782 cm^{-1} to fit experimental spectra (see Figures 6 and 7). Consistent with this finding is the extrapolated 0% GC end point deduced from the natural DNA data. The above results can be of significance in assigning calculated modes to observed Raman bands. Another somewhat surprising observation is the intensity for poly[d(G-C)]·poly[d(G-C)] at 782 cm^{-1}. It is lower than projected from the other DNA data. This result was observed with several independent spectra. It may reflect some unique conformational property for this DNA. The 791-cm^{-1} band was initially assigned to a backbone vibration by Peticolas and collaborators (Erfurth et al., 1975). Although the measurement error of this band's intensities is large, the data are consistent with this interpretation.

800-850-cm^{-1} Region. One of the unexpected observations of the study was the presence of a band around 809 cm^{-1} in the spectra of all the natural and synthetic DNAs. This band cannot be visually detected in spectra from the natural DNAs, poly[d(G-C)]·poly[d(G-C)], and poly[d(T-G)]·poly[d(C-A)]. However, the curve fitting analysis required it to accurately fit each spectra of these DNAs. Figure 5 demonstrates this for *M. luteus* DNA. Figure 5a shows the calculated fit when a band around 809 cm^{-1} was included. Figure 5b displays the result of the curve fitting analysis in the absence of this band. The fitting algorithm attempts to compensate for the absence of the 809-cm^{-1} band by increasing the widths of other bands to 40–50 cm^{-1}. Even with this compensating flexibility, the calculated spectra did not reproduce the experimental spectra. Similar results were obtained for the other DNAs (see paragraph at end of paper regarding supplementary material). We also note that six bands is the least number of bands that fit the data. The 809-cm^{-1} band of the natural DNAs was generally broader than that of the synthetic DNAs and could be fit with a larger number of modes. A Raman peak of high intensity near 809 cm^{-1} is characteristic of an A-type DNA backbone. It has been correlated by experiment (Erfurth et al., 1975) and theory (Lu et al., 1977) with a vibrational mode involving both the deoxyribose group in a C3′-endo ring pucker and the C5′–O–P(O_2^-) atoms.

Figures 6 and 7 display the 800-cm^{-1} region of the AT DNA polymers. The spectra of these DNAs differ from the other DNA spectra between 800 and 850 cm^{-1}. The "809"-cm^{-1} A-family band and "835"-cm^{-1} B-family band are located at 816 and 841 cm^{-1}, respectively, in poly[d(A)]·poly[d(T)]. The curve fitting analysis of poly[d(A-T)]·poly[d(A-T)] spectra shows a requirement for an additional Raman band at 823 cm^{-1} (Figure 7). This band has a width and peak height similar to its neighboring bands. It is not possible to accurately fit this DNA's Raman spectra with only two bands. This was the only DNA we examined that required three bands from 800 to 840 cm^{-1}. Interpretation of this band is postponed until later.

Figure 8 shows band intensity vs. percent GC for the 809-cm^{-1}, 835-cm^{-1} and two other backbone modes. The 816-cm^{-1} band of poly[d(A)]·poly[d(T)] and the 811-cm^{-1} band of poly[d(A-T)]·poly[d(A-T)] are considered as "809"-cm^{-1} bands. The change in intensity with percent GC is small for

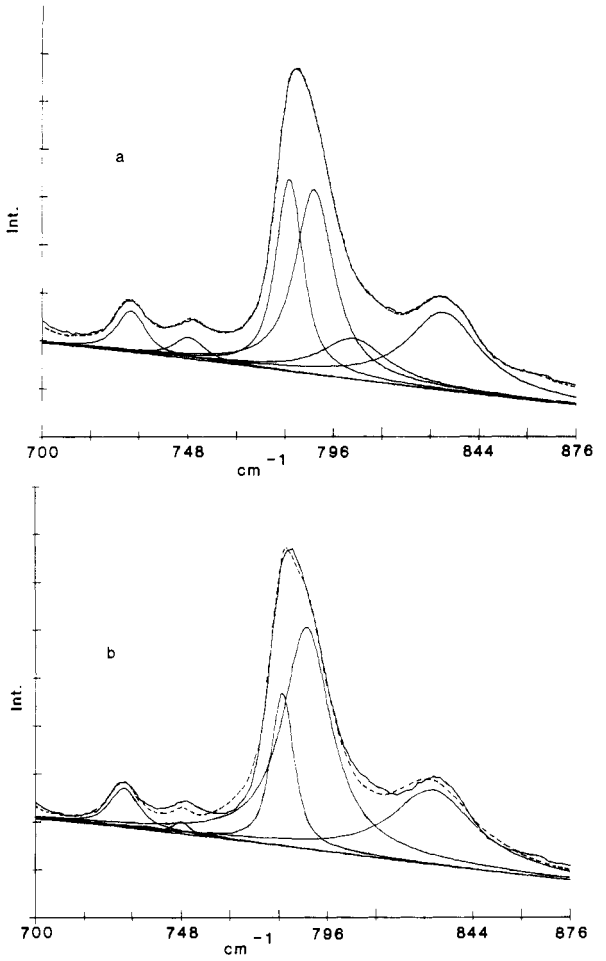

FIGURE 5: Experimental and fitted spectra of *M. luteus* DNA from 700 to 876 cm^{-1}. Solid lines denote experimental spectra, Raman bands, and background curve. Dashed line denotes the sum of background curve and Raman bands. (a) Six bands employed in analysis procedure. (b) Five bands used in analysis procedure. The same fitting criteria were used in both cases.

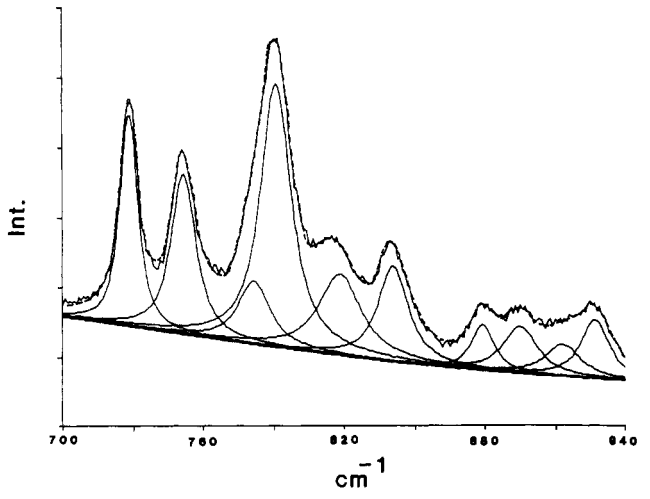

FIGURE 6: Raman spectra of poly[d(A)]·poly[d(T)] and Raman bands and background curve determined from the analysis procedure. Solid lines denote experimental spectra, background curve, and Raman bands. Dashed line denotes sum of background curve and Raman bands.

all of these bands. This is consistent with their being backbone modes. Deviations from expected intensities are observed for poly[d(G-C)]·poly[d(G-C)] at 835 cm^{-1} and for the AT and GC DNA polymers at 924 cm^{-1}.

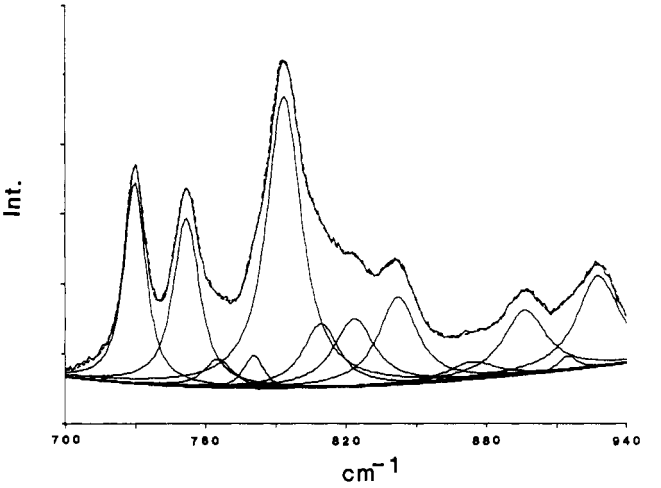

FIGURE 7: Raman spectra of poly[d(A-T)]·poly[d(A-T)] and Raman bands and background curve determined from the analysis procedures. Solid lines denote experimental spectra, background curve, and Raman bands. Dashed line denotes sum of background curve and Raman bands.

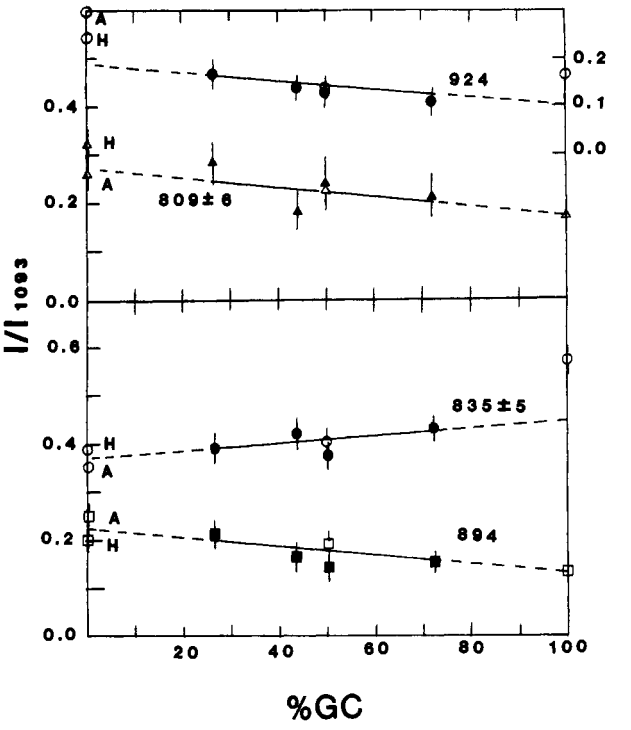

FIGURE 8: Raman intensities vs. percent GC for bands at 809, 835, 894, and 924 cm^{-1}. See Figure 3 legend for symbol description.

Intensity vs. percent GC plots were obtained for a number of bands in the 1000–1600-cm^{-1} region. This portion of the spectra has many overlapping bands. We reiterate that the bands required for this spectral region form a minimum set. Some are likely to correspond to overlapping modes. Although the percent GC dependence of these Raman bands are generally consistent with prior assignments, several exceptions are noted. Bands at or near 1052, 1213, 1237, 1256, 1333, and 1420 cm^{-1} show little change in intensity for all the DNAs. The 1052- and 1420-cm^{-1} bands were assigned to backbone modes (Prescott et al., 1984). The constant intensities of these bands with percent GC reinforce these assignments. The band found near 1213 cm^{-1} was broad and overlapped with the 1237-cm^{-1} band. Both bands were assigned to thymine ring modes by Prescott et al. (1984). A different assignment for the 1237-cm^{-1} peak (cytosine) was made by Chou and Thomas

Table I: Characteristics and Assignments of Raman Bands Observed in both Natural and Periodic DNAs[a]

nominal frequency (cm^{-1})[b]	width at half-height (cm^{-1})[c]	assignment	nominal frequency (cm^{-1})[b]	width at half-height (cm^{-1})[c]	assignment
490	14.0	Ade/Thy[d]	1115	25.0	
499	9.0	Gua, Thy	1143	10.0	Ade/Thy
534	8.0	Ade	1178	16.0	Gua/Cyt
579	7.0	Gua/Cyt	1192	7.0	
596	8.5	Cyt	1213*	28.0	bk/mm
641	11.0	Ade, Cyt	1237*	12–23	bk/mm
670	10.0	Thy	1256	19.0	Cyt, Ade
682.5	11.5	Gua-Rib	1268*	9–21	
729	8.0	Ade, u	1302	13.5	Ade
750	11.5	Thy	1317	12.0	Gua
782	8.0	Cyt, u	1333	14.0	bk/mm
791	14.5	bk	1342	16.0	Ade
809*	24.5	bk	1361	17.0	Gua/Cyt
835*	22.0	bk	1375	15.0	Ade, Gua, Thy
894	20.0	bk	1420	11.0	Rib
924*	19.0	bk	1444	6–20	
998	20.0		1460	10–30	
1013	27.0	Ade/Thy	1488	13.0	Gua, Ade
1052	12.0	bk	1512	7.0	Ade
1067*	26		1575	14	Gua, Ade
1093	16	bk (PO_2^-)			

[a] These bands were observed for most if not all DNAs. A number of bands specific for individual DNA polymers are not listed. [b] Bands that varied in frequency by more than ±2 cm^{-1} among the DNAs are starred marked with an asterisk (*). [c] If the SD of the band width was less than 25% of the average width, then the average value is given. Otherwise, the range is given. [d] A slant (/) means and/or. A comma implies and. Gua, guanine; Cyt, cytosine; Ade, adenine; Thy, thymine; u, unknown; bk, backbone; Rib, deoxyribose; mm, multiple base modes.

(1980) and Strommen and Peticolas (1982). Since the intensity of neither band changes with GC content, it is unlikely that they correspond to vibrations of a single base. A variation of ±6 cm^{-1} was observed for the peaks of these bands among the synthetic DNAs. These bands may result from a backbone mode and/or several base modes. Theory and experiment indicate an antisymmetric phosphate stretch in this region (Lu et al., 1977; Forrest & Lord, 1977).

Several bands assigned to adenine—at 1302, 1342, and 1512 cm^{-1}—show the expected decrease in intensity with increasing percent GC. Large differences occur in the intensities of these bands for poly[d(A)]·poly[d(T)] and poly[d(A-T)]·poly[d(A-T)]. This implies that these adenine modes are sensitive to conformational differences between these DNAs. Table I lists bands observed in the DNAs studied. Assignments are based on this and previous work.

Discussion

The requirement for a band around 809 cm^{-1} in all spectra indicates that a portion of the deoxyribose rings in "B-type DNA" assume a C3′-endo family conformation (throughout the Discussion, we will refer to this A-DNA-type deoxyribose–phosphate mode as a C3′-endo family mode). This conclusion is based on the assignment of the deconvoluted 809-cm^{-1} band to the same backbone mode that produces a large peak at this frequency for A-DNA fibers. The small change in band intensity vs. percent GC is consistent with this assignment. Also, bandwidths are similar to those found for the 835-cm^{-1} backbone band.

The coexistence of the 809- and 835-cm^{-1} bands can be due to the dynamic fluctuation of every deoxyribose ring and/or to two populations of furanose conformations, each one correlated with specific nucleotide sequences. Drew et al. (1981) observed a distribution of furanose conformations in B-DNA oligomer crystals, but with the exception of a guanine base at the 3′ end, only 1 out of 20 internal bases had a furanose pucker close to C3′-endo. NMR studies of various DNA sequences have not yet indicated a population of C3′-endo-type sugar rings (Reid et al., 1983; Assa-Munt & Kearns, 1984; Sarma et al., 1985). These results suggest that the Raman

Table II: Frequencies of Bands in the 800–850-cm^{-1} Region

DNA	C3′-endo family (cm^{-1})	C2′-endo family (cm^{-1})	other band (cm^{-1})
poly[d(A)]·poly[d(T)]	816	841	
poly[d(A-T)]·poly[d(A-T)]	810	842	823
C. perfringens	811	837	
B. subtilis	808	834	
E. coli	805	834	
poly[d(T-G)]·poly[d(C-A)]	807	837	
M. luteus	803	833	
poly[d(G-C)]·poly[d(G-C)]	803	831	

experiments are sampling the dynamic character of all rings, although a small equilibrium population of C3′-endo rings is likely. The intensity of the 809-cm^{-1} band determined from this study as well as from calf thymus DNA in solution is about 20% of the 809-cm^{-1} band in A-DNA calf thymus fibers (Martin & Wartell, 1982). This suggests that 20% of the deoxyribose rings of solution DNA are in the C3′-endo family conformation. The remainder are presumably in the C2′-endo family.

Another observation that is probably related to conformational variability is the influence of percent GC on the frequencies of the nominal 809- and 835-cm^{-1} bands. This has also been noted by others (Thomas & Peticolas, 1983b; Thomas & Benevidis, 1985). Table II shows an upward shift of about 10 cm^{-1} for both bands with increasing percent GC. One explanation for this behavior is that these "backbone" modes actually involve base atom motions (Lu et al., 1979) and are sensitive to base pair type. Alternatively, it may reflect small differences in backbone conformation with percent GC. Evidence for a relationship between the frequency of the 809-cm^{-1} mode and conformation was given by Thomas and Peticolas, (1983a). The frequency of this C3′-endo band was correlated with the sugar torsion angle δ of RNA oligomers. Raman studies of B-type DNA crystal structures and normal mode analysis should illuminate this issue.

Arnott et al. (1983) proposed a heteronomous secondary structure for both high- and low-humidity fibers of poly[d(A)]·poly[d(T)]. One strand, probably poly[d(A)], had

C3′-endo sugar puckers and backbone torsion angles similar to those of A-type DNA. The poly[d(T)] strand had C2′-endo sugar puckers and a backbone similar to the canonical B-type conformation. If this conformation occurs in solution, the fraction of deoxyribose rings with an A-like pucker would be expected to be greater than is observed for other DNAs. Although the frequency of the 816-cm^{-1} band of poly[d(A)]·poly[d(T)] implies unique characteristics for this DNA's backbone conformation, the intensity of this band is similar to that of the C3′-endo family bands of all other DNAs (Figure 8). The validity of relating the intensity of this band to the fraction of C3′-endo sugars is indicated by a comparison of A-type DNA fibers and duplex RNAs. These nucleic acids have C3′-endo family bands with nearly the same intensity relative to the 1099-cm^{-1} band (1.6–1.65), even though their peaks differ by 6–8 cm^{-1} (Prescott et al., 1984; Thomas & Hartman, 1973). If poly[d(A)]·poly[d(T)] was 50% C3′-endo, one could expect the relative intensity at 816 cm^{-1} to be about 0.8 instead of 0.32. The width of the 816-cm^{-1} band is narrower than that of the 809-cm^{-1}-type bands of natural DNAs (20 vs. 25–33 cm^{-1}), but it is similar to the widths of other synthetic DNAs.

Thomas and Peticolas (1983a) have shown that the 816-cm^{-1} peak sharpens and increases by ~10% when the temperature of poly[d(A)]·poly[d(T)] is reduced to 0 °C. Jolles et al. (1985) has recently obtained evidence that at 0 °C the adenine strand adopts an A-family structure as suggested by Arnott et al. (1983). Resonance Raman intensities of three adenine modes in poly[d(A)]·poly[d(T)] and other RNA and DNA polymers were compared. The hypochromism of these bands at 0 °C relative to 80 °C implied that the structure of the adenine strand of poly[d(A)]·poly[d(T)] is more like that of poly[r(A)] and poly[r(A)]·poly[r(U)], than poly[d(A)] or poly[d(A-T)]·poly[d(A-T)]. Taken together, the Raman studies indicate that at 0 °C poly[d(A)]·poly[d(T)] has features characteristic of a heteronomous structure. Even at this temperature, however, the relative intensity of the C3′-endo band is less than expected for a rigid heteronomous structure. At 25 °C, the intensity measurements at 816 and 841 cm^{-1} do not indicate a significantly higher ratio of C3′-endo/C2′-endo conformers than for other DNAs. On a Raman time scale, the sugar pucker of poly[d(A)]·poly[d(T)] is more dynamic than indicated by the heteronomous model. NMR studies are also in disagreement with the heteronomous model (Sarma et al., 1985).

In addition to the anomalous frequency of the C3′-endo family band, the intensities of several base vibrations of poly[(dA)·poly[d(T)] differ from the natural DNA extrapolation. The adenine band at 729 cm^{-1} and the thymine bands at 669 and 750 cm^{-1} have slightly higher intensities than the line extrapolated from the natural DNA data (Figures 3 and 4). Base modes at 1302 and 1375 cm^{-1} show lower intensities. Linear dichroism studies of poly[d(A)]·poly[d(T)] in solution indicate that its base pair propeller twist is significantly different from other DNA sequences (Edmondson & Johnson, 1985). The Raman intensity results probably reflect these differences in adenine and thymine modes.

The Raman spectra of poly[d(A-T)]·poly[d(A-T)] has several unique features. It was the only DNA that required three bands in the 800–850-cm^{-1} region. These three bands suggest the presence of three discrete backbone bands. The absence of the "extra" 823-cm^{-1} band in poly[d(A)]·poly[d(T)] argues against it being a base vibration. Although a novel proposal, previous studies indicate some uncertainty as to the backbone of poly[d(A-T)]·poly[d(A-T)]. NMR studies by Assa-Munt and Kearns (1984) and Jenkins et al. (1985) showed that the solution structure of poly[d(A-T)]·poly[d(A-T)] was consistent with a right-handed B-type conformation in which both adenine and thymine have C2~-endo-type sugar puckers. In comparing the NMR studies with our Raman data, it is important to note that these two methods measure signals on different time scales. A Raman scattering event takes place in about 10^{-12}–10^{-13} s, while NMR measurements using the two-dimensional nuclear Overhauser effect average over at least 10^{-6}. If, for example, the deoxyribose ring pucker is fluctuating between conformational states at a rate r, with $10^7 < r < 10^{11}$ s^{-1}, NMR measurements will see an average over two (or more) states whereas Raman spectroscopy can delineate populations of discrete states. The occurrence of three Raman backbone modes is thus not necessarily in conflict with the NMR data. Assa-Munt and Kearns (1984) observed an interaction between two different adenine H2 resonances. This implied a cross-strand proximity of two adenines in different environments and suggested different conformation coexist within poly[d(A-T)]·poly[d(A-T)]. Other evidence for multiple backbone conformations in this polymer comes from the X-ray diffraction studies of Millane et al. (1984). At low relative humidity, a fiber of poly[d(A-T)]·poly[d(A-T)] was observed to have a structural repeat of six nucleotide pairs.

The intensities of base vibrations in poly[d(A-T)]·poly[d(A-T)] also indicate unique features. The 1342- and 1512-cm^{-1} adenine bands have intensities that are greater than those of poly[d(A)]·poly[d(T)] and the line extrapolated from the natural DNAs. A lack of knowledge about the detailed atomic motions of these adenine modes precludes further interpretation. We note though that these two adenine modes show no intensity changes upon DNA denaturation, whereas other adenine bands at 1375 and 1512 cm^{-1} do (Erfurth & Peticolas, 1975). Benevides and Thomas (1985) have also shown that the adenine base in poly[d(A-T)]·poly[d(A-T)] has anomalous properties with respect to deuterium exchange.

The remaining two synthetic DNAs examined in this study, poly[d(T-G)]·poly[d(C-A)] and poly[d(G-C)]·poly[d(G-C)], are clearly of the B type. Most Raman bands have frequencies and intensities consistent with the natural DNA data. A few exceptions are worth noting. Poly[d(G-C)]·poly[d(G-C)] has a higher intensity at 835 cm^{-1} than extrapolated from the natural DNAs (Figures 8). This may indicate an increased population of C2′-endo furanose rings due to the increased stacking interaction in this DNA. A pTpT crystal with well-defined C2′-endo sugar puckers has a peak at 835 cm^{-1} with an intensity much higher than that found for B-DNA fibers (Thomas & Peticolas, 1983a). This observation indicates that this band's intensity is sensitive to the population of deoxyribose rings with a C2′-endo pucker. Stacking may also account for the decrease in the 782-cm^{-1} cytosine band. For poly[d(T-G)]·poly[d(C-A)], the bands that have significant deviations from the expected intensities are adenine and thymine bands (669, 750, 1302, and 1342 cm^{-1}). This implies that the A·T pair of this polymer differs in some way from an average A·T in natural DNAs.

Added in Proof

Recently, G. J. Thomas and collaborators have also obtained evidence for multiple Raman bands in the 800–850-cm^{-1} region for DNA in solution (Thomas et al., 1986).

Acknowledgments

We acknowledge Dr. Ian Gatland for assistance in the initial stages of development of the analysis program. We thank Dr. Bruce Jenkins and Dr. James Alderfer for their generous gift

of poly[d(T-G)]·poly[d(C-A)].

Supplementary Material Available

Figures 1S–4S showing the background curve and 18 bands that fit the 640–1150-cm^{-1} region, the fitted spectra for five and six bands in the *C. perfringens* DNA 700–876-cm^{-1} region, and intensity vs. percent GC plots for eight bands from 1050 to 1530 cm^{-1} (6 pages). Ordering information is given on any current masthead page.

Registry No. Poly[d(A)]·poly[d(T)], 24939-09-1; poly[d(T-G)]·poly[d(C-A)], 27732-52-1; poly[d(A-T)]·poly[d(A-T)], 26966-61-0; poly[d(G-C)]·poly[d(G-C)], 36786-90-0.

References

Arnott, S., Chandrasekaran, R., Hall, I. H., & Puigjaner, L. C. (1983) *Nucleic Acids Res. 11*, 4141.

Assa-Munt, N., & Kearns, D. R. (1984) *Biochemistry 23*, 791.

Benevides, J. M., & Thomas, G. J., Jr. (1985) *Biopolymers 24*, 667.

Chou, C. H., & Thomas, G. J., Jr. (1977) *Biopolymers 16*, 765.

Dickerson, R. E., Drew, H. R., Conner, B. N., Wing, R. M., Frateni, A. V., & Kopka, M. L. (1982) *Science (Washington, D.C.) 216*, 475.

Drew, H. R., Wing, R. M., Takana, T., Broka, T., Tanaka, S., Itakura, K., & Dickerson, R. E. (1981) *Proc. Natl. Acad. Sci. U.S.A. 78*, 2179.

Edmondson, S. P., & Johnson, W. C., Jr. (1985) *Biopolymers 24*, 825.

Englander, S. W., & Kallenbach, N. (1983) *Q. Rev. Biophys. 16*, 521.

Erfurth, S. C., & Peticolas, W. L. (1975) *Biopolymers 14*, 247.

Erfurth, S. C., Bond, P. J., & Peticolas, W. L. (1975) *Biopolymers 14*, 1245.

Fidor, S. P., Starr, P. A., & Spiro, T. G. (1984) *Biophys. J. 45*, 119a.

Forrest, G., & Lord, R. C. (1977) *J. Raman Spectrosc. 6*, 32.

Hagerman, P. (1981) *Biopolymers 20*, 1503.

Hartman, K. A., Lord, R. C., & Thomas, G. J., Jr. (1973) in *Physico-Chemical Properties of Nucleic Acids* (Duchesne, J., Ed.) pp 1–89, Academic, New York.

Horowitz, D. S., & Wang, J. C. (1984) *J. Mol. Biol. 173*, 75.

Jenkins, B., & Alderfer, J. L. (1985) *Biophys. J. 47*, 331a.

Jolles, B., Laigle, A., Chinsky, L, & Turpin, P. Y. (1985) *Nucleic Acids Res. 13*, 2075.

Klysik, J., Stirdivant, S., Larson, J. E., Hart, P. A., & Wells, R. D. (1981) *Nature (London) 290*, 671.

Lord, R. C., & Thomas, G. J., Jr. (1967) *Spectrochim. Acta, Part A 23A*, 2551.

Lu, K.-C., Prohofsky, E. W., & Van Zandt, L. L. (1977) *Biopolymers 16*, 2491.

Lu, K.-C., Van Zandt, L. L., & Prohofsky, E. W. (1979) *Biophys. J. 28*, 27.

Marquardt, J. W. (1963) *J. Soc. Ind. Appl. Math. 11*, 431.

Martin, J. C., & Wartell, R. M. (1982) *Biopolymers 21*, 499.

Milane, R. P., Walker, J. K., Arnott, S., Chandrasekaran, R., & Birdsall, D. L. (1984) *Nucleic Acids Res. 12*, 5475.

Mirau, P. A., & Kearns, D. R. (1983) in *Structure and Dynamics: Nucleic Acids and Proteins* (Clementi, E., & Sarma, R. H., Eds.) pp 227–239, Adenine, Albany, NY.

Mirau, P. A., & Kearns, D. R. (1985) *Biopolymers 24*, 711.

Nishimura, Y., Hirakawa, A. Y., & Tsuboi, M. (1978) *Adv. Infrared Raman Spectrosc. 5*, 217.

Nishimura, Y., Tsuboi, M., & Sato, T. (1984) *Nucleic Acids Res. 12*, 6901.

Pohl, F. M., Ranade, A., & Stockburger, M. (1973) *Biochim. Biophys. Acta 335*, 85.

Prescott, B., Steinmetz, W., & Thomas, G. J., Jr. (1984) *Biopolymers 23*, 235.

Reid, D. G., Salisbury, S. A., Bellard, S., Shakked, Z., & Williams, D. H. (1983) *Biochemistry 22*, 2019.

Rich, A., Quigley, G. J., & Wang, A. H.-J. (1981) in *Biomolecular Stereodynamics* (Sarma, R. H., Ed.) pp 35–52, Adenine, Albany, NY.

Sarma, M. H., Gupta, G., & Sarma, R. H. (1985) *J. Biomol. Struct. Dyn. 2*, 1057.

Shakked, D., Rabinovich, D., Kennard, O., Cruse, W. B. T., Salisbury, S. A., & Viswamitra, M. A. (1983) *J. Mol. Biol. 166*, 183.

Shore, D., & Baldwin, R. L. (1983) *J. Mol. Biol. 170*, 957.

Thomas, G. J., Jr., & Hartman, K. C. (1973) *Biochim. Biophys. Acta 312*, 311.

Thomas, G. J., Jr., & Kyogoku, Y. (1977) *Pract. Spectrosc. 1C*, 717.

Thomas, G. A., & Peticolas, W. L. (1983a) *J. Am. Chem. Soc. 105*, 986.

Thomas, G. A., & Peticolas, W. L. (1983b) *J. Am. Chem. Soc. 105*, 993.

Thomas, G. J., Jr., & Benevides, J. M. (1985) *Biopolymers 24*, 1101.

Thomas, G. J., Jr., Benevides, J. M., & Prescott, B. (1986) in *Biomolecular Stereodynamics* (Sarma, R. H., Ed.) Vol. III, Adenine, Albany, NY.

Strommen, D. P., & Peticolas, W. L. (1982) *Biopolymers 21*, 969.

Wang, A. H.-J., Quigley, G. J., Kolpak, G., van der Marel, J. H., van Boom, J. H., & Rich, A. (1980) *Science (Washington, D.C.) 211*, 171.

Wartell, R. M., & Benight, A. S. (1982) *Biopolymers 21*, 2069.

Wartell, R. M., Harrell, J. T., Zacharias, W., & Wells, R. D. (1983) *J. Biomol. Struct. Dyn. 1*, 83.